THERMAL STABILITY OF HALLOYSITE BY HIGH-PRESSURE DIFFERENTIAL THERMAL ANALYSIS

Sheryl L. Johnson, Stephen Guggenheim, and A. F. Koster van Groos

Department of Geological Sciences, University of Illinois at Chicago
Chicago, Illinois 60680

Abstract—Platy (Te Puke, New Zealand), cylindrical (Spruce Pine, North Carolina), and spherical (North Gardiner mine, Huron, Lawrence County, Indiana) halloysite samples were analyzed by high-pressure differential thermal analysis (HP-DTA) to determine the effect of morphological and chemical differences on their respective thermal stability. In halloysite, these morphological differences imply structural features. The metastable phase relations of each are analogous to those of kaolinite. At 1 bar, the platy, cylindrical, and spherical samples showed peak temperatures (maximum deflection in the dehydroxylation endotherm) of 560°, 578°, and 575°C, respectively, whereas at about 600 bars the peak temperatures were 622°, 655°, and 647°C. At low pressures the observed reaction is related to dehydroxylation: halloysite (H) = metahalloysite (MH) + vapor (V), whereas higher pressures produce melting reactions, either H + V = metaliquid (ML) for conditions of $P(H_2O) = P(total)$, or H + MH = ML for $P(H_2O) < P(total)$. The PT conditions of the invariant point, H + MH + ML + V, for each system are: Te Puke, 612° ± 4°C, 25 ± 7 bars; Spruce Pine, 657 ± 2°C, 30 ± 7 bars; North Gardiner, 652° ± 2°C, 34 ± 7 bars. The lower thermal stability of the Te Puke sample may be related to its higher iron content, although additional data are necessary to confirm that it is not related also to the platy structure. Furthermore, morphological differences between the cylindrical and spherical varieties appear to have had little effect on the energy required to dehydroxylate these halloysite structures. Exceptionally high values obtained for the dehydroxylation enthalpies using the van't Hoff equation, compared with values derived using other methods, may be explained by a 10–15-bar excess in the intracrystalline H_2O fugacity during dehydroxylation. Intracrystalline fugacity is defined here as the H_2O fugacity within crystallites and is not related to the partial pressure of H_2O around individual particles.

Key Words—Dehydroxylation, Halloysite, High-pressure differential thermal analysis, Morphology, Phase relations, Thermal stability.

INTRODUCTION

Halloysite is a dioctahedral 1:1 layer silicate that has an ideal composition of $Al_2Si_2O_5(OH)_4 \cdot nH_2O$, where n = 0 to 2. Interlayer water is weakly bound and, depending on humidity, may be lost at temperatures of 50°C (Hofmann *et al.,* 1934) or less (D. L. Bish, personal communication, Los Alamos National Laboratory, Los Alamos, New Mexico), yielding a product similar to kaolinite, $Al_2Si_2O_5(OH)_4$. With additional heating to about 600°C, halloysite dehydroxylates to a disordered layer-like structure containing some residual hydroxyls (Pampuch, 1966). This structure is comparable to metakaolinite and, for convenience, it is referred to as "metahalloysite" in this paper, although the term has been used previously to indicate a variety of phases.

Because halloysite contains interlayer water but is otherwise chemically and structurally similar to kaolinite, many attempts (Ross and Kerr, 1934; Alexander *et al.,* 1943; Brindley and Robinson, 1946; Bates *et al.,* 1950; Bramao *et al.,* 1952; Farmer and Russell, 1964; Chukhrov and Zvyagin, 1966) have been made to demonstrate a clear distinction between halloysite and kaolinite. Alexander *et al.* (1943) and Bates *et al.* (1950) showed that, unlike the platy structure of kaolinite, halloysite commonly displays a cylindrical (cyl-

inder-like) morphology, although other morphologies, such as plates and spheres, have been observed as well (Kunze and Bradley, 1964; Askenasy *et al.,* 1973; McKee *et al.,* 1973; Dixon and McKee, 1974). As a result, many workers (Bates *et al.,* 1950; Bates, 1959; Radoslovich, 1963; Hope and Kittrick, 1964; Tazaki, 1982; Noro, 1986) have attempted to evaluate the relation between chemistry, structure, environment of formation, and the various morphologies of halloysite.

After removal of interlayer water, halloysite requires hydrogen bonding across the interlayer region similar to other 1:1 structures, including kaolinite. Differences in the hydrogen bonding network between collapsed (7-Å) halloysite and kaolinite, however, can be expected. For cylindrical and spherical halloysite, the number and orientation of the hydrogen bonds must differ from kaolinite (and from platy halloysite) because of the different ways of stacking, resulting in either cylindrical or spherical morphology. Furthermore, if a small net negative charge exists on the 1:1 layers in halloysite due to a small amount of Al tetrahedral substitution, as suggested recently by S. W. Bailey (personal communication, Department of Geology and Geophysics, University of Wisconsin-Madison, Madison, Wisconsin), the hydrogen bonding configuration across the interlayer region should differ also between platy (7-Å) halloysite and kaolinite. It is of

477

interest, therefore, to evaluate the manner in which halloysite dehydroxylates and to contrast its behavior with that of kaolinite.

Halloysite, like kaolinite, has hydroxyl groups associated with the Al octahedral sites. Hydroxyls in halloysite are located both within the 1:1 layer and at the atomic planes adjacent to the interlayer. Stone (1952) and Weber and Roy (1965a, 1965b), from dehydroxylation studies of halloysite and kaolinite using differential thermal analysis (DTA), found that the dehydroxylation temperature of halloysite is slightly less than that of kaolinite, both at low pressures (0.006 to 1 bar: Stone, 1952) and at higher pressures (1 to 680 bars: Weber and Roy, 1965a). Weber and Roy (1965a) observed that an increase in pressure to about 27.5 bars raised the dehydroxylation temperature markedly, but that a further pressure increase reduced the reaction temperature. This apparently unique change in the dehydroxylation reaction was not understood, but they suggested that "some mechanism, presumably the catalytic effect of water facilitates structural reorganization at much lower temperatures." In a study of the dehydroxylation of kaolinite, Yeskis *et al.* (1985) presented evidence that this reorganization, which was related to the apparent reduction of reaction temperature, is the result of a different reaction involving the metastable melting of kaolinite in the presence of excess vapor.

The enthalpy of the dehydroxylation reaction is related to the difference in bonding energy of OH, less the energy involved in the formation of new bonds. For halloysite, the enthalpy of dehydroxylation is related to the number and strength of the hydrogen bonds in the structure. Because halloysite is a 1:1 structure, the hydrogen network involves both the inner-hydroxyl H as well as the H at the layer surfaces. Calculations of dehydroxylation enthalpies (ΔH_{dh}) by Weber and Roy (1965b) on the basis of the peak area of the DTA signal showed not only a greater average ΔH_{dh} for halloysite (172 kJ/mole), but also a greater range in ΔH_{dh} than for kaolinite (163 kJ/mole). Stone (1952), however, using a modified van't Hoff equation, calculated a lower ΔH_{dh} for halloysite, about 150 kJ/mole, although for kaolinite he found ΔH_{dh} = 570 kJ/mole.

The study presented here reports a high-pressure differential thermal analysis (HP-DTA) of the various morphological forms of halloysite in order to determine the dehydroxylation enthalpy as a function of morphology, pressure, temperature, and $P(H_2O)$. In halloysite, the morphological features of plates, cylinders, and spheres imply structural features.

EXPERIMENTAL PROCEDURE

Apparatus

The HP-DTA system (Koster van Groos, 1979) consisted of a copper sample holder, which accommodated three sample capsules. Gold foil was used in an extrusion technique to form capsules 7 mm in length, 3 mm in diameter, and 110 mg in weight. A 1-mm deep re-entry well was formed at the base of each capsule to position the Pt-Pt$_{90}$Rh$_{10}$ thermocouple at the center of the sample volume. One capsule contained about 20 mg of reference material (α-Al$_2$O$_3$), and two capsules each contained 20 mg of sample. Preparation of the sample material included mixing with 20 wt. % pure quartz (St. Peter Sandstone) for 15 min in a SPEX mixer/mill. The quartz was added as an internal temperature standard using the low-high quartz inversion (Koster van Groos and ter Heege, 1973). The samples were stored in a desiccator over a saturated solution of Mg(NO$_3$)$_2 \cdot$6H$_2$O (55% RH).

Before insertion of the capsules into the copper sample holder, the cells were coated with TiO$_2$ to insure both electrical and thermal insulation. The completed assembly was sealed within an internally heated pressure vessel, similar to the one described by Holloway (1971), and mounted horizontally.

The temperature range for each run was 30°–700°C; the heating rate was 20°C/min. The temperature of the sample was obtained from the reference capsule thermocouple and corrected for deviations by using the differential temperature (ΔT). The correction was usually 1°–2°C, with corrected temperatures accurate to $\pm$1°C. The HP-DTA signals were recorded on the 20- and 50-μV range of a Kipp recorder, resolving ΔT to 0.02°C and 0.05°C, respectively. Pressure, using argon as the pressure medium, was measured by calibrated Bourdon-type Heise gauges and is accurate to within 0.5%. Separate gauges for low and high pressures covered ranges of 0–68 bars and 0–1000 bars, respectively. To determine the effect of water vapor pressure on the reaction, the samples were run under two conditions. About 50 runs were made with open-system conditions, $P(H_2O) < P(total)$. A second series of 30 runs was made with water added to the sample and the capsule welded shut, so that $P(H_2O) = P(total)$. Of these, almost half failed because of leaks and were discarded.

To determine the effect of the heating rate, one sample (from Spruce Pine, North Carolina) was run at 7°/min and 1 bar. The peak temperature, defined as the temperature at the maximum deflection of the dehydroxylation endotherm, was 562°C (cf. peak temperature of 560°C at a heating rate of 20°C/min). Thus, the heating rate did not seriously affect the peak temperatures.

Materials

A platy, a cylindrical, and a spherical halloysite variety were examined. The platy sample from Te Puke, New Zealand, was described by Hughes (1966) as a 10-Å, water-sorted product from weathering and/or hydrothermal alteration of rhyolite and andesite.
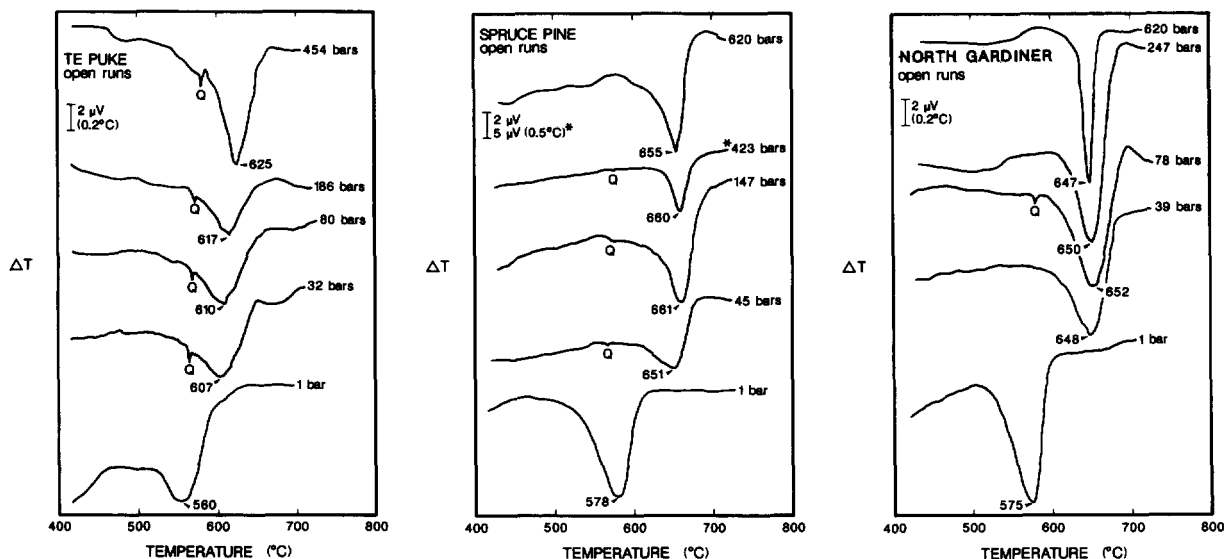
Figure 1. Open-capsule high-pressure differential thermal analysis curves at selected pressures. Arrows indicate peak temperatures. Q denotes quartz peak.

McKee *et al.* (1973) described the morphology as platy, with some bends in the layers and with minor amounts of cylindrical material present. The second sample was a cylindrical, 7-Å halloysite (Arrowhead mine, Spruce Pine, North Carolina; Ward's Natural Science Establishment, Rochester, New York). The spherical variety was a 10-Å halloysite from the North Gardiner mine, Huron, Lawrence County, Indiana. The spherical halloysite appeared to have formed during extensive weathering along an unconformity, underlain by limestone and overlain by a sandstone that contained ferruginous bands (Sunderman, 1963). The samples are herein referred to as Te Puke, Spruce Pine, and North Gardiner. The Spruce Pine and North Gardiner samples were analyzed (Table 1) by X-ray fluorescence techniques. The analyses of the Te Puke sample are from Churchman and Theng (1984) and Hughes (1966). The main chemical difference between the three halloysite specimens is the significant amount of Fe in the Te Puke sample and the relatively large amounts of Na_2O and P_2O_5, probably as a sodium phosphate, in the Spruce Pine sample. Scanning electron microscopy showed that the average grain size is 3–5 μm (in plan) for the Te Puke sample, 3–5 μm in length for the Spruce Pine sample, and about 1 μm in diameter for the North Gardiner sample.

After the HP-DTA runs were completed, the products were analyzed using petrographic and Debye-Scherrer and (Scintag) diffractometer X-ray powder diffraction methods. X-ray powder diffraction data of selected run products showed the presence of metahalloysite and poorly crystalline tridymite. Mullite was present in some runs also.

RESULTS

HP-DTA curves of selected open-capsule runs for each sample are shown in Figure 1. The curves usually show a quartz endotherm due to the low-high transition of the quartz that was added as a temperature calibrant. From 1 to 40 bars, peak temperatures due to halloysite dehydroxylation increased as much as 70°C. With a further increase in pressure to about 450–620 bars, the peak temperature remained nearly con-

Table 1. Chemical analyses of Te Puke, Spruce Pine, and North Gardiner halloysite.

Oxides	Te Puke (platy) 1	Te Puke (platy) 2	Spruce Pine (cylindrical) 3	North Gardiner (spherical) 4
SiO_2	44.82	41.03	43.73	46.15
Al_2O_3	36.74	32.92	36.16	40.06
TiO_2	0.37	0.10	0.00	0.00
Fe_2O_3[1]	3.40	3.60	0.23	0.10
MnO	n.a.[2]	n.a.	0.01	0.10
MgO	<0.01	0.06	0.00	0.00
CaO	<0.01	0.04	0.39	0.09
Na_2O	0.01	0.10	2.07	0.07
K_2O	0.05	<0.10	0.36	0.10
P_2O_5	<0.01	n.a.	4.92	0.10
H_2O-	n.a.	8.85	n.a.	n.a.
H_2O+[3]	15.8	13.10	n.a.	n.a.
Total	101.2	99.90	87.52	86.69

[1] Total iron as Fe_2O_3.
[2] Not analyzed.
[3] Based on loss on ignition at 1500°C.
Column 1. X-ray fluorescence, Churchman and Theng (1984).
Column 2. Wet-chemical analysis, Hughes (1966).
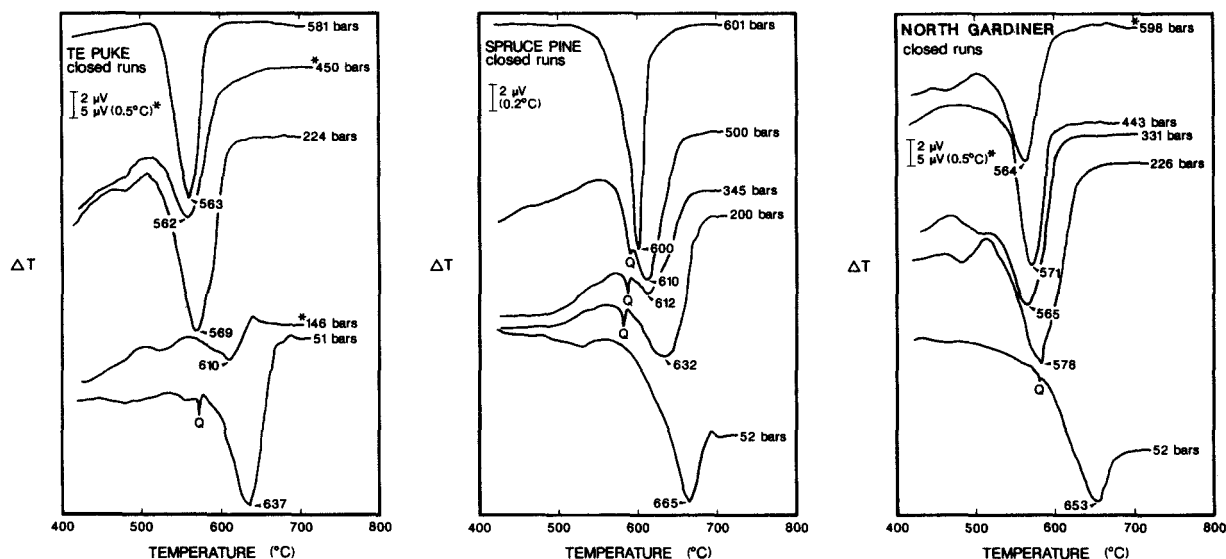Columns 3, 4. X-ray fluorescence, T. A. Vogel, analyst.

Figure 2.   Closed-capsule high-pressure differential thermal analysis curves at selected pressures. Arrows and Q as in Figure 1.

stant or decreased slightly at the higher pressures. Peak width, defined as the temperature difference between the first deviation of the signal from the baseline and its return, generally decreased with pressure. This effect was especially apparent for the spherical halloysite. Figure 2 illustrates the changes in peak temperature and peak width for closed-capsule runs. All three halloysite specimens showed a decrease in peak temperature and peak width with pressure for the closed capsule runs.

The pressure and temperature data for the dehydroxylation reaction of each halloysite are given in Table 2. Both the extrapolated onset temperature (intersection of the tangent of the peak limb with the base line) and the peak temperature are listed. For open-capsule runs, the Spruce Pine and North Gardiner samples gave similar results. At 1 bar, the peak temperature of both samples was near 575°C, whereas higher pressures (600 bars) gave temperatures near 650°C. Peak temperatures for the Te Puke sample were lower, ranging from 560° to 625°C. Furthermore, unlike the other two samples, the Te Puke sample temperatures showed more scatter.

In closed-capsule runs, the peak temperatures decreased as much as 75°C with a pressure increase from 50 to 200 bars, but a further increase in pressure did not significantly affect the temperature. The Te Puke and North Gardiner samples gave similar peak temperatures. At about 50 bars, these were 637° and 653°C, respectively. With increasing pressure, the difference in temperature became smaller, and the reaction for both samples was at 565°C at 600 bars. The reaction temperature of the Spruce Pine sample was higher,

ranging from 665°C at 50 bars to 600°C at 600 bars. Several runs showed a weight-loss during the experiments, indicating leakage. In these runs the reaction temperature increased substantially, because of the lowering of the partial pressure of H_2O.

DISCUSSION

Three reactions involving halloysite are suggested by the data of this study. One reaction was encountered in open capsules at <40 bars and had a strong temperature dependency on pressure. A second reaction was noted for open capsules at pressures >40 bars; the effect of pressure on the temperature of this reaction was negligible. A third reaction was noted in closed capsules at pressures >40 bars, and, for this reaction, the temperature decreased with increasing pressure. These reactions are analogous to a series of reactions established for kaolinite (Yeskis *et al.*, 1985). As such, they are consistent with the chemical and structural similarities of kaolinite and halloysite. Reaction (1) is a dehydroxylation reaction, halloysite (H) = metahalloysite (MH) + vapor (V). In this reaction, the vapor phase is probably pure H_2O (Yeskis *et al.*, 1985). Reaction (2), halloysite (H) + metahalloysite (MH) = metaliquid (ML), is a melting reaction in which vapor is absent. Because this reaction is vapor-absent, the pressure effect on the reaction temperature is small. Reaction (3), halloysite (H) + vapor (V) = metaliquid (ML), represents a vapor-saturated melting reaction. The metaliquid (ML) is believed to be a quasi-layerlike structure derived from halloysite or metahalloysite, with a partial loss of periodicity within the layers. This mosaic arrangement produces a liquid-like character, which

Table 2. High-pressure differential thermal analysis data for Te Puke, Spruce Pine, and North Gardiner halloysite.

Te Puke (platy)				Spruce Pine (cylindrical)				North Gardiner (spherical)			
Wt. % H_2O	Onset temperature (°C)	Peak temperature (°C)	Peak pressure (bars)	Wt. % H_2O	Onset temperature (°C)	Peak temperature (°C)	Peak pressure (bars)	Wt. % H_2O	Onset temperature (°C)	Peak temperature (°C)	Peak pressure (bars)
0	503	560	1	0	534	578	1	0	521	575	1
10	502	581	3	10	530	608	3	0	538	607	3
10	510	600	7	0	537	627	7	20	563	617	4
0	493	598	9	10	591	637	10	10	552	621	7
20	527	597	12	10	560	640	15	0	545	625	10
20	539	605	17	10	562	637	16	20	572	635	15
10	543	625	18	20	558	640	18	10	567	638	16
10	522	620	20	10	580	643	19	10	558	633	18
10	496	611	21	0	562	642	20	10	568	637	19
10	550	617	22	10	568	645	21	0	584	635	20
20	533	607	32	20	598	653	29	10	586	637	21
20	537	607	50	20	585	651	45	20	582	648	39
20	493	600	71	10	621	653	79	20	598	652	78
20	533	610	80	20	627	655	80	10	605	650	247
20	568	617	186	10	603	658	81	20	620	647	620
0	587	625	454	20	616	661	141	0[1]	592	653	52
20	580	622	536	20	591	661	147	0[1]	521	578	226
10[1]	582	637	51	20	645	660	264	10[1]	507	565	331
10[1]	562	610	146	20	639	660	423	0[1]	514	571	443
10[1]	514	569	224	0	613	655	620	10[1]	523	567	451
10[1]	525	564	280	0[1]	613	665	52	5[1]	521	564	598
0[1]	525	562	450	10[1]	569	632	200				
5[1]	520	563	581	15[1]	555	612	345				
				10[1]	567	610	483				
				10[1]	560	610	500				
				10[1]	545	600	601				

[1] Closed-capsule runs.

allows the variable water content, as is required by the several reactions involving ML. Assuming the system metahalloysite–H_2O to be binary, an invariant point (I, Figure 3) having the assemblage H + MH + ML + V must be present. On the basis of Schreinemaker's rule, additional reactions are required, and their relative positions in PT space can be inferred. Thus, a melting reaction MH + V = ML extends from the invariant point to the metastable melting temperature at one atmosphere. A second melting reaction involving halloysite (H = ML + V) emanates from the invariant point to higher pressures and temperatures. The H_2O content of the metaliquid produced in this reaction near the invariant point is less than that of halloysite, but increases with pressure and becomes equal to that of halloysite at the singular point S. From this point, two additional reactions occur at higher pressures: the reaction H = ML, in which the H_2O content of the metaliquid is constant and equal to that of halloysite, and the reaction H + V = ML, in which the H_2O content of the metaliquid continues to increase.

In open-capsule runs, the peak temperatures of the Spruce Pine and North Gardiner samples were similar, but the reaction temperatures for the Te Puke sample were consistently lower by 30°–40°C. These data result in a *first* approximation (see below for further discus-

sion) of the location of the invariant point for the Te Puke sample at 612° ± 4°C and 18 ± 3 bars, of the Spruce Pine sample at 657° ± 2°C and 24 ± 2 bars, and of the North Gardiner sample at 652° ± 2°C and 27 ± 2 bars.

The reduction in temperature of the dehydroxylation reaction of the Te Puke sample relative to the other samples indicates a significant decrease in its thermal stability. The reduced thermal stability may be an expression of the reduction in field-strength of the octahedrally coordinated cation in the halloysite structure, i.e., the Fe-for-Al substitution in the Te Puke sample. As was observed by Noro (1986), however, the platy morphology of halloysite is related to the Fe content as well. Therefore, the decrease in thermal stability of the platy sample may be related to a combination of chemistry and/or morphology (i.e., the nature of the interlayer bonding).

The peak temperatures and pressures for open-capsule runs, which defined the dehydroxylation reaction H = MH + V, were used to calculate ΔH_{dh}, following the (integrated) van't Hoff equation: $\Delta H = nR(\ln P_2 - \ln P_1)/(1/T_2 - 1/T_1)$, in which n is the number of H_2O molecules released in the reaction, and assuming that the fugacity coefficient of H_2O equals one (see, e.g., Stone, 1952; Anderson, 1977). If the volume of H_2O vapor released during dehydroxylation was sufficiently
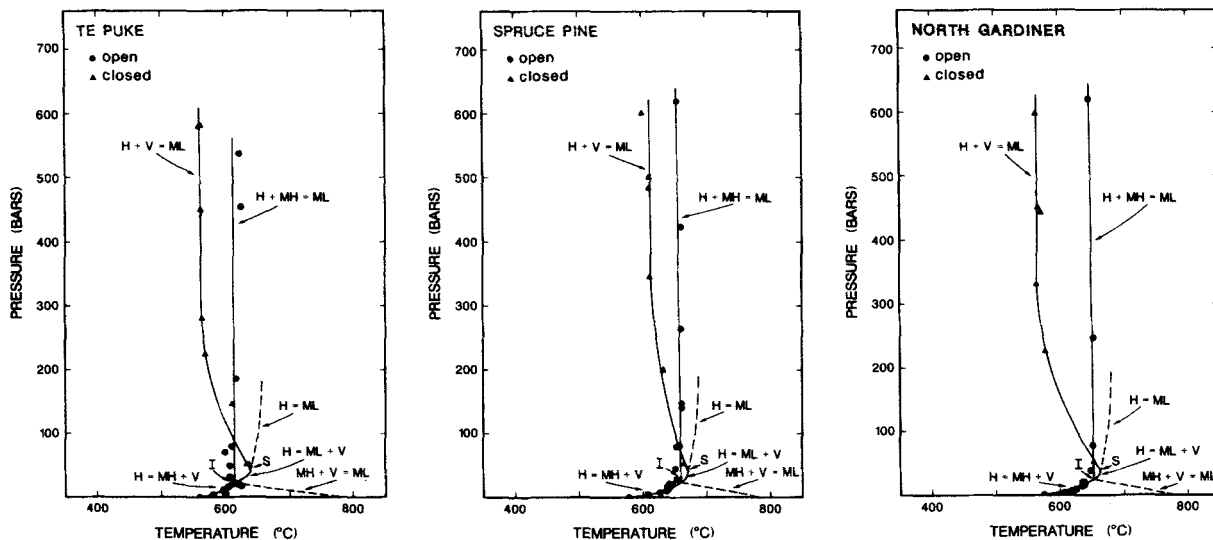
Figure 3.   PT relations in the system metahalloysite-H_2O. Symbols: H = halloysite; MH = metahalloysite; ML = metaliquid; V = vapor; I = invariant point; S = singular point.

large to flush all argon away from the sample, $P(H_2O)$ was equal to P(total). Using the one-atmosphere data and the PT conditions of the invariant point, the following ΔH_{dh} values were obtained: 630 ± 40 kJ/mole (Te Puke and North Gardiner samples) and 584 ± 30 kJ/mole (Spruce Pine sample). The error is related to the uncertainty of the PT conditions of the dehydroxylation reaction at 1 bar and the invariant reaction.

The dehydroxylation enthalpy values as determined above appear to be high. In comparison, Weber and Roy (1965b) obtained $\Delta H_{dh} = 170$ kJ/mole using the peak area of the DTA signal in experiments involving pure H_2O pressures. If their PT data at 1 bar and 27.5 bars, as derived from the extrapolated onset temperatures, are used in the van't Hoff equation, however, a similar high ΔH_{dh} (550 kJ/mole) results. Furthermore, Stone (1952) obtained a ΔH_{dh} value of 150 kJ/mole based on onset temperatures and the van't Hoff equation. The onset temperatures he used, especially at the lower pressures, were obtained from a very small deviation of the differential temperature on his DTA curves at a much lower temperature than the onset of the peak itself. Such low temperatures, of course, produce low enthalpy values.

Similar inconsistencies exist for kaolinite. Using the data of Yeskis *et al.* (1985) in the van't Hoff equation gave a ΔH_{dh} value of 550 kJ/mole. A determination of ΔH_{dh} by Stone (1952) following the van't Hoff equation and lower pressure DTA data under conditions of $P(total) = P(H_2O)$, yielded $\Delta H_{dh} = 585$ kJ/mole. In contrast, Weber and Roy (1965b), using the area of the DTA peak, found values of 160 ± 10 kJ/mole for kaolinite. Using their data at 1 atmosphere and at 27.5 bars in the van't Hoff equation, however, resulted in

$\Delta H_{dh} = 500$ kJ/mole. As was noted by Stone (1952), such high values seem to be quite unreasonable.

The dehydroxylation enthalpies, as derived using the van't Hoff equation under different experimental conditions are consistently unreasonably high, which suggests a systematic error that may be related to the kinetics of the system. A likely cause is that the fugacity of H_2O within the solid phases is substantially higher during the experiments than was measured using the external pressure. Therefore, the differences of these enthalpy values may be reconciled by assuming that during the heating cycle, when dehydroxylation commenced, the intracrystalline fugacity of H_2O increased and exceeded the external fugacity of H_2O. Considering that the H_2O molecules must diffuse through the crystalline structure before exit, this mechanism appears reasonable. We emphasize that the internal crystalline fugacity differs from partial pressures around the crystallites; it involves the quality of crystallinity, crystallite size, and other properties that affect diffusion within a crystallite. An excess of 10–15 bars in the intracrystalline H_2O fugacity is sufficient to reconcile the differences in the enthalpy values.

The effect of the elevated intracrystalline H_2O fugacity on the PT conditions of the invariant point is difficult to assess. The temperature of the invariant point was derived from the temperature-insensitive reaction (2) and, therefore, is reasonably precise. The pressure of this reaction is constrained (1) by the values as determined in this study and by the investigation of Weber and Roy (1965b) and (2) by the addition of the 10–15 bars excess pressure, as discussed above. Therefore, the best estimates of the PT conditions of the invariant point for the three halloysite samples are:

Te Puke, $612° \pm 4°C$ and 25 ± 7 bars; Spruce Pine, $657° \pm 2°C$ and 30 ± 7 bars; and North Gardiner, $652° \pm 2°C$ and 34 ± 7 bars.

These reactions represent metastable equilibrium reactions. The equilibrium decomposition temperature of the kaolin-group minerals is about 400°C (Roy and Osborn, 1954). Therefore, additional phases that were identified by XRD, such as mullite and quartz, are not considered in this discussion. These phases are assumed to represent part of the stable assemblage for halloysite compositions at these PT conditions (e.g., Roy and Osborn, 1954), and, as such, have no role in the metastable phase relations considered here.

SUMMARY AND CONCLUSIONS

The metastable phase relations of halloysite and kaolinite are analogous. Small differences in thermal stability between different halloysite samples, however, were observed. The behavior of the North Gardiner and Spruce Pine halloysite samples at low H_2O fugacities appears identical within error. In the presence of excess H_2O, however, the North Gardiner kaolinite melted at significantly lower temperatures. The Te Puke halloysite had a substantially lower thermal stability. The decreased thermal stability may be due to the higher Fe content of this sample or to the platy morphology (or both). Previous work (Noro, 1986) indicates that an increase in the Fe^{3+} content in halloysite may cause the platy morphology. It may be impossible, therefore, to separate the two factors.

The van't Hoff equation, which is commonly applied to determine enthalpies of devolatilization (e.g., in dehydroxylation or other reactions involving volatiles), should be used with caution in dynamic systems. Using this equation, unreasonably high values for the enthalpy of dehydroxylation of halloysite were obtained from this study, as well as from data of other studies, when compared with values using other methods. A similar effect is seen for kaolin-group minerals. If intracrystalline H_2O fugacities in these minerals can exceed external H_2O fugacities by 10–15 bars during dehydroxylation, the differences are reconciled. Although at high total pressures the effect is minor, at low pressures substantial errors may result.

REFERENCES

Alexander, L. T., Faust, G. T., Hendricks, S. B., Insley, H., and McMurdie, H. F. (1943) Relationship of the clay minerals halloysite and endellite: *Amer. Mineral.* **28**, 1–18.

Anderson, G. M. (1977) Fugacity, activity and equilibrium constant: in *Application of Thermodynamics to Petrology and Ore Deposits*, Mineralogical Association of Canada Short Course Handbook **2**, H. J. Greenwood, ed., 17–37.

Askenasy, P. E., Dixon, J. B., and McKee, T. R. (1973) Spheroidal halloysite in a Guatemalan soil: *Soil Sci. Amer. Proc.* **37**, 799–803.

Bates, T. F. (1959) Morphology and crystal chemistry of 1:1 layer lattice silicates: *Amer. Mineral.* **44**, 78–114.

Bates, T. F., Hildebrand, F. A., and Swineford, A. (1950) Morphology and structure of endellite and halloysite: *Amer. Mineral.* **35**, 463–484.

Bramao, L., Cady, J. G., Hendricks, S. B., and Swerdlow, M. (1952) Criteria for the characterization of kaolinite, halloysite, and a related mineral in clays and soils: *Soil Science* **73**, 273–287.

Brindley, G. W. and Robinson, K. (1946) Randomness in the structures of kaolinitic clay minerals: *Trans. Faraday Soc.* **42**, 198–205.

Chukhrov, F. V. and Zvyagin, B. B. (1966) Halloysite, a crystallochemically and mineralogically distinct species: in *Proc. Int. Clay Conf., Jerusalem, 1966, Vol. 1*, L. Heller and A. Weiss, eds., Israel Prog. Sci. Transl., Jerusalem, 11–25.

Churchman, G. J. and Theng, B. K. G. (1984) Interactions of halloysites with amides: Mineralogical factors affecting complex formation: *Clay Miner.* **19**, 161–175.

Dixon, J. B. and McKee, T. R. (1974) Internal and external morphology of tubular and spheroidal halloysite particles: *Clays & Clay Minerals* **22**, 127–137.

Farmer, V. C. and Russell, J. D. (1964) The i.r. spectra of layer silicates: *Spectrochim. Acta* **20**, 1149–1173.

Hofmann, U., Endell, K., and Wilm, D. (1934) Röntgenographische und kolloidchemische Untersuchungen über Ton: *Angew. Chem.* **47**, 539–547.

Holloway, J. R. (1971) Internally heated pressure vessels: in *Research for High Pressure and Temperature*, G. C. Ulmer, ed., Springer-Verlag, New York, 217–258.

Hope, E. W. and Kittrick, J. A. (1964) Surface tension and the morphology of halloysite: *Amer. Mineral.* **49**, 859–866.

Hughes, I. R. (1966) Mineral changes of halloysite on drying: *New Zealand J. Sci.* **9**, 103–113.

Koster van Groos, A. F. (1979) Differential thermal analysis of the system $NaF-Na_2CO_3$ to 10 kbar: *J. Phys. Chem.* **83**, 2976–2978.

Koster van Groos, A. F. and ter Heege, J. P. (1973). The high-low quartz transition up to 10 kilobar pressure: *J. Geol.* **81**, 281–286.

Kunze, G. W. and Bradley, W. F. (1964) Occurrence of a tabular halloysite in a Texas soil: in *Clays and Clay Minerals, Proc. 12th Natl. Conf., Atlanta, Georgia, 1963*, W. F. Bradley, ed., Pergamon Press, New York, 523–527.

McKee, T. R., Dixon, J. B., Whitehouse, G., and Harling, D. F. (1973) Study of Te Puke halloysite by a high resolution electron microscope: *Abstr. 31st Ann. Electron Microscopy Soc. Amer. Meeting, New Orleans, Louisiana, 1973*, 200–201.

Noro, H. (1986) Hexagonal platy halloysite in an altered tuff bed, Komaki City, Aichi Prefecture, central Japan: *Clay Miner.* **21**, 401–415.

Pampuch, R. (1966) Infrared study of thermal transfor-

mation of kaolinite and the structure of metakaolin: *Polska Akad. Nauk Prace Mineral.* **6**, 53–70.

Radoslovich, E. W. (1963) The cell dimensions and symmetry of layer-lattice silicates, VI. Serpentine and kaolin morphology: *Amer. Mineral.* **48**, 368–378.

Ross, C. S. and Kerr, P. F. (1934) Halloysite and allophane: *U.S. Geol. Surv. Prof. Pap.* **185-G,** 135–148.

Roy, R. and Osborn, E. F. (1954) The system Al_2O_3-SiO_2-H_2O: *Amer. Mineral.* **39,** 853–885.

Stone, R. L. (1952) Differential thermal analysis of kaolin-group minerals under controlled partial pressures of H_2O: *J. Amer. Ceram. Soc.* **35,** 90–99.

Sunderman, J. A. (1963) Mineral deposits at the Mississippian-Pennsylvanian unconformity in southwestern Indiana: M.S. thesis, Indiana University, Bloomington, Indiana, 115 pp.

Tazaki, K. (1982) Analytical electron microscopic studies of halloysite formation processes—Morphology and composition of halloysite: in *Proc. Int. Clay Conf., Bologna, Pavia, 1981,* H. van Olphen and F. Veniale, eds., Elsevier, Amsterdam, 573–584.

Weber, J. N. and Roy, R. (1965a) Dehydroxylation of kaolinite, dickite, and halloysite: *J. Amer. Ceram. Soc.* **48,** 309–311.

Weber, J. N. and Roy, R. (1965b) Dehydroxylation of kaolinite, dickite and halloysite: Heats of reaction and kinetics of dehydration at $P(H_2O) = 15$ psi: *Amer. Mineral.* **50,** 1038–1045.

Yeskis, D., Koster van Groos, A. F., and Guggenheim, S. (1985) The dehydroxylation of kaolinite: *Amer. Mineral.* **70,** 159–164.